4-18-2023

Machine learning technique for damage detection of rails on steel railroad bridges subjected to moving train load

Md Masnun Rahman
The University of Texas Rio Grande Valley

Mohsen Amjadian
The University of Texas Rio Grande Valley, mohsen.amjadian@utrgv.edu

Mahesh Pokhrel
The University of Texas Rio Grande Valley

Constantine Tarawneh
The University of Texas Rio Grande Valley, constantine.tarawneh@utrgv.edu

Recommended Citation

Md. Masnun Rahman, Mohsen Amjadian, Mahesh Pokhrel, and Constantine Tarawneh "Machine learning technique for damage detection of rails on steel railroad bridges subjected to moving train load", Proc. SPIE 12487, Nondestructive Characterization and Monitoring of Advanced Materials, Aerospace, Civil Infrastructure, and Transportation XVII, 124870R (18 April 2023); https://doi.org/10.1117/12.2661723

Machine learning technique for damage detection of rails on steel railroad bridges subjected to moving train load

Md Masnun Rahman[a], Mohsen Amjadian[*a], Mahesh Pokhrel[a], Constantine Tarawneh[b]
[a] Department of Civil Engineering, The University of Texas Rio Grande Valley, 1201 W University Dr, Edinburg, TX 78539.
[b] Department of Mechanical Engineering, The University of Texas Rio Grande Valley, 1201 W University Dr, Edinburg, TX 78539.

ABSTRACT

Rail is one of the key elements of the railway system, and its role is to transmit the wheel load to the track bed and guide the train cars along the track. Rail is susceptible to rolling contact fatigue and wear due to being repeatedly subjected to the moving load of the train. This can eventually result in broken-rail damage and train derailment, which if happens on a railroad bridge, it can severely damage the bridge, such as the structural failure of the Tempe Town Lake steel railroad bridge in July 2020 that costed $11 million to repair. Therefore, early detection of defects in rail-bridge system may prevent a critical accident with irreversible damage. The objective of this paper is to use classification-based machine learning techniques to detect broken-rail damage in an open-deck railroad bridge by measuring its acceleration response under the moving load of the train for different speeds. For this purpose, the two-dimensional Finite Element (2D FE) model of a given railroad bridge is created using OpenSEESPy package, which is a Python-3 interpreter of OpenSEES. The changes in the acceleration response due to the damaged rail compared to the undamaged (healthy) rail are characterized by using the Hilbert-Huang Transform in both the time and frequency domains and quantified by defining energy and phase damage indices. The data collected from the 2D FE model are used to train and test several machine learning (ML) classifiers including the Support Vector Machine (SVM), K-Nearest Neighbor (KNN), and Decision Tree (DT) algorithms. The results from the data-analytic study show an acceptable level of precision of these classifiers in identifying the damage to the rail-bridge system.

Keywords: Defected rail, Steel railroad bridge, Damage detection, Finite-element modelling, Time-frequency domain, and Machine learning.

1. INTRODUCTION

The US railway system is one of the largest in the world, with over 140,000 miles of track [1]. It is used to transport a wide range of goods, including coal, oil, and agricultural products, and passengers on long-distance and commuter trains. Despite the growth of other forms of transportation, such as highways and air travel, railways remain an important part of the US transportation network due to their conveniences, safety, and efficiency. Railroad bridges are essential parts of the railway network, providing a crucial link between different zones of the network. These bridges are designed to carry heavy loads of train cars, passengers, and cargo across rivers, valleys, and other bodies of water. However, many of these bridges were built in the early 1900s and are now reaching the end of their useful lifespan [2]. In addition, the increase in heavy freight traffic has put additional strain on these ageing structures. Open-deck railroad bridges are more susceptible to structural damage due to the moving load of train as the wheel impact load is much higher in these bridges compared to the bridges with ballasted deck.

A train derailment can be described as an event when one or more of the train's wheels leave the tracks, causing the train to become unbalanced and unable to continue moving safely. A variety of factors, such as irregularities in the rail, broken rails, buckling of the rails, improper support at the rails, excessive speed, etc., can cause this failure. A train derailment that occurs on an old bridge that is not well maintained may result in severe damage as well as the collapse of the bridge, as such events are recently being witnessed at an alarming rate all over the US railway network due to the ageing of the old centurion bridges. To mention a few recent events, in September 2021, two train cars derailed from the Wabash River

[*]mohsen.amjadian@utrgv.edu; phone (956)665-5880

near downtown Lafayette [3]. On July 2020, during a railway derailment on a bridge over Tempe Town Lake, the bridge collapsed and caught fire, resulting in a tremendous amount of repairing cost [4]. In May 2022, another train derailment occurred near the Arkansas River bridge, causing traffic to back up across the intersections [5]. And just recently, in September 2022, near Hampton, Iowa, a Union Pacific train derailed, impacting approximately 44 train cars and spilling asphalt into a creek that caused irreversible environmental damage [6].

Early detection of a damaged rail can help reduce the chances of such incidents prior to an accident, saving thousands of lives as well as minimizing financial loss [7]. But detecting such a defect in a rail is complex and burdensome for this enormous amount of rail tracks. Mostly the condition monitoring of the rails is done manually with visual inspections that are sometimes erroneous and do not provide the actual cause of damage. There are some non-destructive testing (NDT) methods to analyze and quantify the damage in rails, such as ultrasonic testing [8], Wavelet-based technique [9], optical rail surface crack detection method [10], Impact-echo testing method [11], and ML-based techniques.

This paper aims to develop a 2D FE model from an actual bridge located in Cocke County, Tennessee using the Open System for Earthquake Engineering Simulation (OpenSEES) and classify the different damage scenarios in the rail-bridge system from the datasets obtained from the recorded acceleration signals. Three popular ML algorithms for the classification will be used: Support Vector Machine (SVM), K-Nearest Neighbor (KNN), and Decision Tree (DT) algorithms. The classification model will determine the best parameters to get the highest accuracy in determining the three damaged conditions of the rail-bridge system: healthy: H (Level 0), moderately damaged: D1 (Level I), and severely damaged: D2 (Level II).

2. FINITE ELEMENT MODEL

2.1 Gulf Fork Big Creek railroad bridge

The Gulf Fork Big Creek railroad bridge, constructed in 1919, is owned by Norfolk Southern Railway and is located in Cocke County, Tennessee. The bridge can be categorized as a Warren truss that consists of 6 spans, each of 8 m (26 ft) length, totaling length of 48 m (156 ft). The railroad bridge carries about 17 megatons of freight traffic per year. Traffic consists of loaded and unloaded unit trains and mixed freight and intermodal trains [12]. The actual photograph of the bridge is shown in Figure 1.

Figure 1. Gulf Fork Big Creek railroad bridge [12].

2.2 Bridge modelling in OpenSEESPy

The FE modeling of given rail-bridge system shown in Figure 1 was done by OpenSEESPy using python 3.9 interpreter [13]. For this analysis, only a 2D section of one side of the railroad bridge was considered to reduce complications in modeling the moving load and its interaction with the rail-bridge system.

Figure 2 shows the 2D FE model created in OpenSEESPy. Only the key members of the superstructure (i.e., lower and upper flexural chords and diagonal members) of the rail-bridge system are considered in the study; the other members, such as abutment and bearing components, are disregarded for the sake of simplicity. The end support of the bridge at the East side was modelled as a roller in which the translational motions in x- and y-directions are restrained, whereas the end support at the West side was modelled as a roller in which the translational motion in the y-direction is restrained. For the

lower and upper chords, box type profiles were considered, and channels type profiles were considered for the diagonal members. For the vertical members, I shaped profiles were considered as per the existing drawing details of the Gulf Fork Big Creek railroad bridge [14], [15]. The mid-section vertical and diagonal members were modeled as truss elements where no end bending and torsional moments were applied, while the lower and upper chords were modeled as flexural beams to carry the effects of moving load. Furthermore, it is assumed that all the primary members of the bridge are connected at the junction of their centerlines that pass through the centroid of their cross sections to simplify the complicated features of steel joints in the railroad bridge without sacrificing the accuracy of the FE model.

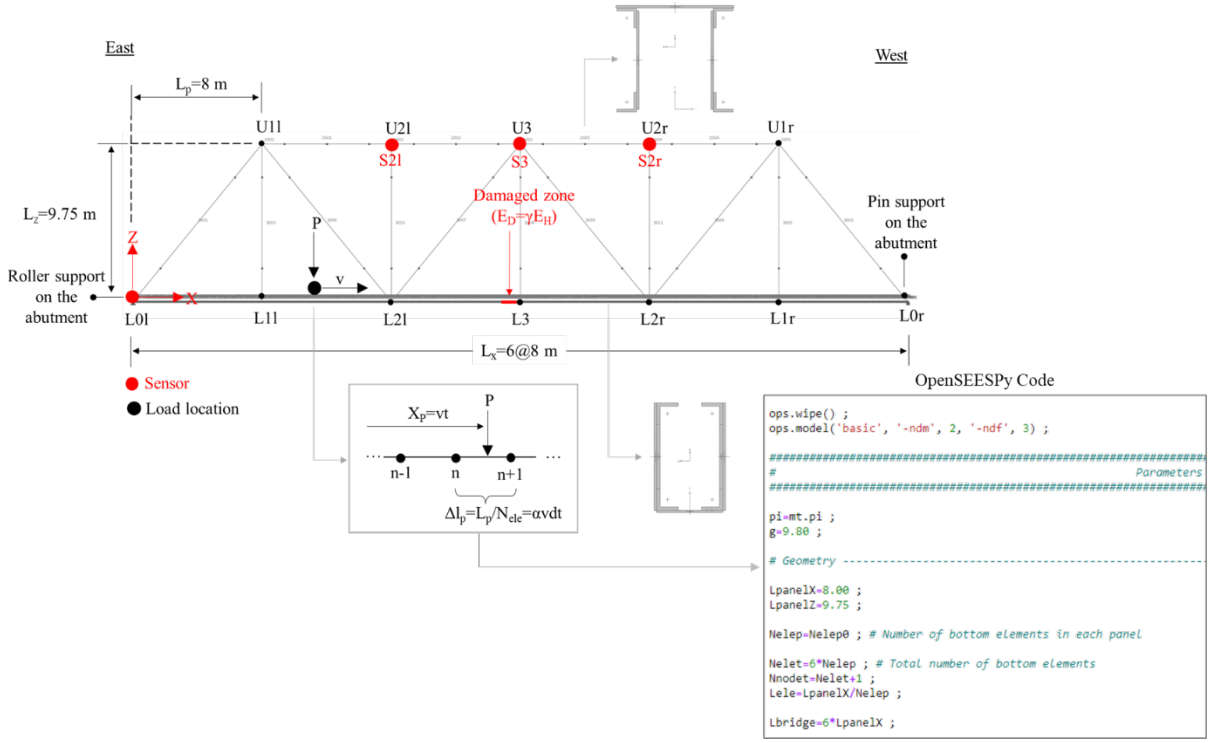

Figure 2. 2D FE model of Gulf Fork Big Creek railroad bridge in OpenSEESPy.

All the members are made of steel with the modulus of elasticity E_s=29000 ksi, which are assumed to behave elastically under the moving load. A moving point load is run for all the nodes covering the full length of bridge. Three sensors were placed at joints U2l, U3, and U2r, which generated the acceleration data for the dynamic analysis. The magnitude of moving point load was taken as 200 kN (the axle load of a typical train in the US) with a constant speed ranging from v=5 m/s to v=100 m/s, where the low speeds demonstrate the static response of the bridge under the moving load (approximately when v<10 m/s).

2.3 Damage modeling

There are several possible causes of damage in a rail-bridge system, including wear and tear from regular use and fatigue degradation, overloading or exceeding the bridge's load capacity, structural design flaws or inadequate construction materials. For all these reasons, the bridge loses its stiffness over time. The defects in the rail can be categorized as broken rail, irregularities in rail, and buckling of rail [16]. In this study, the damage is considered as broken rail, and to model this damage, a small portion of the member L2l-L3 (the load path on the lower chords) next to joint L3, was considered as the damaged zone as shown in Figure 2.

The damage is represented by a change in the modulus of elasticity of steel material used for modeling the rail-bridge system as E_D=γE_H where E_H and E_D denote the modules of elasticity of member in the healthy and damage cases, respectively, and γ represents the extent of damage (γ<1) [17]. In this study, we define three damage cases (see Figure 1): (1) no damage (healthy): γ=1.0, (2) moderate damage (damage level I): γ=0.5, and (3) severe damage (damage level II): γ=0.075.

2.4 Free vibration analysis

A free vibration analysis was carried out to determine the mode shapes and natural frequencies of the railroad bridge's FE model. Figure 3 compares the mode shapes and natural frequencies of the first three modes of the railroad bridge for the case: healthy (H) to those in the case: damage level II (D_2). It is seen that by increasing the level of damage, the first and second mode shapes of the bridge change slightly, while this change is not that obvious for the third mode (and higher modes). Figure 3(b) shows that the damage zone acts as a hinge in the second mode. The natural frequency of the first mode in case H is 9.24 Hz and in case D_2, it is 9.07 Hz indicating a 2% reduction in the natural frequency of the railroad bridge due to the imposed damage.

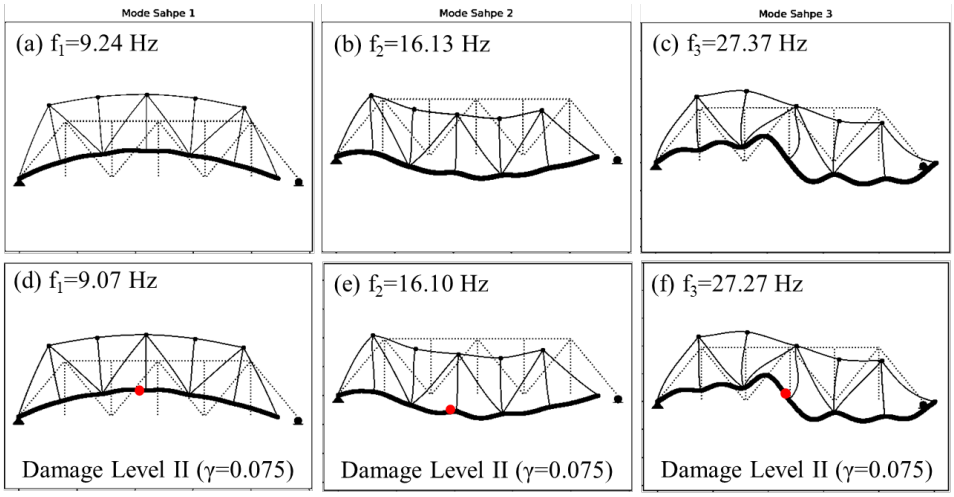

Figure 3. Mode shapes and natural frequencies of the first three modes of the railroad bridge for the case: Healthy (H) (a, b, and c) compared to those in the case: damage level II (D_2) (d, e, and f).

2.5 Transient dynamic analysis

The time history response of the bridge is very sensitive to the value of time step dt and the number of elements N_{ele} used to define the motion of load P=200 kN with the constant speed v. For this reason, a sensitivity analysis is performed to find the optimized values of dt and N_{ele} to optimize the computation time and numerical accuracy of the FE model. In this analysis, the Rayleigh's damping method is used to define the damping in the rail-bridge system, where the critical damping ratio is assumed to be 2.5%.

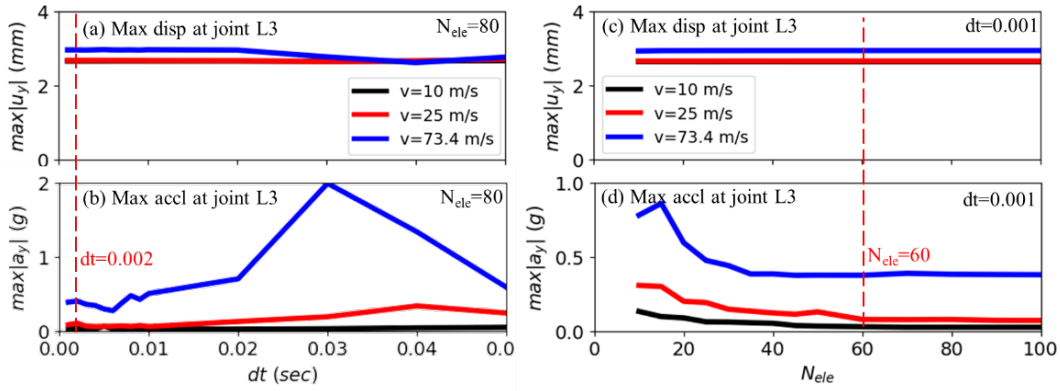

Figure 4. Variation of the maximum displacement and acceleration of the midpoint of the railroad bridge with dt (a and b) and N_{ele} (c and d).

Figures 4(a) and (b) show the variations of the maximum displacement and acceleration of joint L3 of the railroad bridge with dt (time step) under the moving load P=200 kN for v=10 m/s, 25 m/s and 73.4 m/s while assuming that N_{ele}=80. It is seen that with the decrease of dt the dependency of the maximum responses of the bridge on dt is reduced, indicating an

increase in the accuracy of the numerical results. The optimum value of the time step is about dt=0.002 s. However, in this study, this value is taken to be dt=0.001 s. Figures 4(c) and (d) show the variations of the maximum displacement and acceleration of joint L3 with N_{ele} (number of elements) under the moving load P=200 kN for v=10 m/s, 25 m/s and 73.4 m/s by assuming that dt=0.001 s. It is seen that the maximum acceleration is more sensitive than the maximum displacement to the change in N_{ele}. This sensitivity is significantly decreased for N_{ele}>60, as shown in Figure 4(d). In this study, it is assumed that N_{ele}=80.

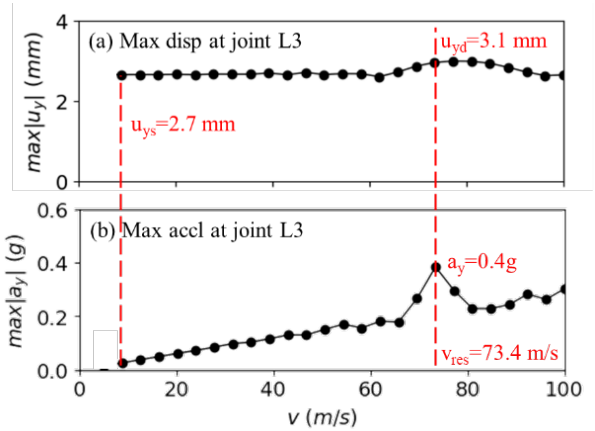

Figure 5. Variation of the maximum displacement (a) and acceleration (b) of the midpoint of the railroad bridge with the speed of moving load.

Figures 5(a) and (b) show the variations of maximum displacement and acceleration of joint L3 with the speed of moving load to find the resonance speed of railroad bridge. From these figures, it can be concluded that the resonance speed of the railroad bridge for a single moving load is about v=73.4 m/s resulting in the maximum displacement 3.1 mm and the maximum acceleration 0.4g. The dynamic amplification factor (DAF) of the displacement response is obtained as $DAF_D=u_{ys}/u_{yd}$=1.15, indicating 15% increase in the displacement response of the railroad bridge under the given moving load.

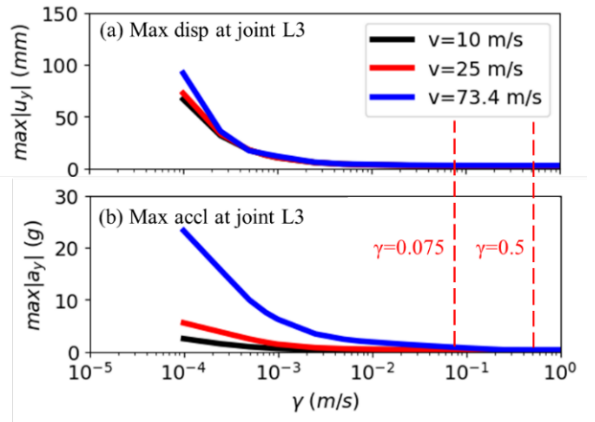

Figure 6. Variation of the maximum displacement (a) and acceleration (b) of the midpoint of the railroad bridge with the damage factor for speeds v=10 m/s, 25 m/s, and 73.4 m/s.

Figures 6(a) and (b) show the variations of maximum displacement and acceleration of joint L3 with the damage factor γ varying from 0.0001 to 1.0 (no damage). It is seen that for those values of γ less than 0.001, the maximum displacement and acceleration responses of railroad bridge significantly increase with the decrease of γ. This is indication of structural instability in the truss when γ<0.001. To model a realistic damage scenario at joint L3, two different values γ=0.5 (moderate damage) and γ=0.075 (severe damage) are considered as previously discussed in section 2.3.

3. DAMAGE MEASUREMENT

3.1 Hilbert-Huang transform

The Hilbert-Huang transform (HHT) is an empirically based data-analysis tool for conducting time-frequency analysis of non-stationary and non-linear signals. The complicated implications hidden in the non-stationary and non-linear time series data can be effectively uncovered by HHT in both the time and frequency domains that otherwise cannot be revealed by traditional data analysis tools such as Fast Fourier Transform (FFT) [7], [18]. The signals recorded by accelerometers on a railroad bridge with the passage of a train are examples of non-stationary time series data which can be described in terms of time, frequency, energy, and phase.

The HHT of acceleration signal is computed in two steps: (1) the empirical mode decomposition (EMD) and (2) the Hilbert spectral analysis (HSA). In the first step, the acceleration signal is decomposed into a finite number of intrinsic mode functions (IMFs). Here, an IMF, as a counterpart to the simple harmonic functions, represents a simple oscillatory signal with variable amplitude and frequency as functions of time. Each IMF signal must satisfy the following conditions [19]: (1) the number of extrema and the number of zero-crossings in the data signal must be either equal or differ at most by one, and (2) the mean value of envelope defined by the local maxima and the envelope specified by the local minima is zero. As per these conditions, each IMF signal is mono-component and has a well-acted Hilbert Transform (HT). Therefore, the acceleration signal $\ddot{u}(t)$ is represented as follows:

$$\ddot{u}(t) = \sum_{i=1}^{M} \ddot{x}_i(t) + \ddot{x}_0(t) \tag{1}$$

where, $\ddot{x}_i(t)$ is the i-th IMF signal and $\ddot{x}_0(t)$ is the residue. The signal has a single positive instantaneous frequency defined by the derivative of its phase function.

In the second step, the analytic signal $\ddot{z}_i(t)$ is defined for the i-th IMF signal as follows,

$$\ddot{z}_i(t) = \ddot{x}_i(t) + j\ddot{y}_i(t) \tag{2}$$

where j is the imaginary unit and $\ddot{y}_i(t)$ is the HT of i-th IMF signal that is defined as [18],

$$\ddot{y}_i(t) = H\{\ddot{x}_i(t)\} = \frac{1}{\pi}\int_0^{t_N} \frac{\ddot{x}_i(\tau)}{t-\tau} d\tau \tag{3}$$

The analytic signal $\ddot{z}_i(t)$ is a complex-valued function which can be expressed into the following polar form,

$$\ddot{z}_i(t) = a_i(t)\exp\left[j\phi_i(t)\right] \tag{4}$$

where, $a_i(t)$ and $\phi_i(t)$ are the instantaneous amplitude and phase of the signal that can be given as,

$$a_i(t) = \sqrt{\ddot{x}_i^2(t) + \ddot{y}_i^2(t)},\ \phi_i(t) = \tan^{-1}\left(\frac{\ddot{y}_i(t)}{\ddot{x}_i(t)}\right) \tag{5}$$

The first derivative of $\phi_i(t)$ gives the instantaneous circular frequency of i-th IMF signal as,

$$\omega_i(t) = \frac{d\phi_i(t)}{dt} \tag{6}$$

The instantaneous energy of i-th IMF signal with its intensity is given by,

$$E_i(t) = |a_i(t)|^2 \tag{7}$$

Finally, the time-frequency distribution of instantaneous amplitude in the 3D space in terms of three parameters t, ω_i, and a_i is called Hilbert spectrum (HS) for i-th IMF and is denoted by $H_i(\omega, t)$. The HS of original acceleration signal $\ddot{u}(t)$ is defined as,

$$H(\omega, t) = \sum_{i=1}^{M} H_i(\omega, t) \tag{8}$$

3.2 Damage quantification

The damage to the rail-bridge system defined by γ in section 2.3 is quantified by the two damage indices DI_E and DI_ϕ describing the changes in the energy and phase of acceleration signals recorded by sensors U2l, U3, and U2r. Here, DI>0 indicates the presence of damage in the bridge, and DI=0 indicates no damage (Healthy). The energy damage index DI_E is defined as [7], [20],

$$DI_E = \left| 1 - \frac{(S_E)_D}{(S_E)_H} \right| \times 100 \tag{9}$$

where S_E is the area below the energy function E(t) that is defined as,

$$E(t) = \int_0^{\omega_n} H^2(\omega, t)\, d\omega \tag{10}$$

The phase damage index DI_ϕ is defined as,

$$DI_\phi = \left| 1 - \frac{(\bar{\phi})_D}{(\bar{\phi})_H} \right| \times 100 \tag{11}$$

where $\bar{\phi}$ is the average of the instantaneous phase of recorded acceleration signal taken over time and of IMFs and can be expressed as:

$$\bar{\phi} = \frac{1}{NM} \sum_{i=1}^{M} \sum_{n=1}^{N} \phi_i(t_n) \tag{12}$$

The extracted features of the signal above, such as frequency, amplitude, energy, and phase, can be effectively utilized for pattern recognition and anomaly detection in the recorded signals.

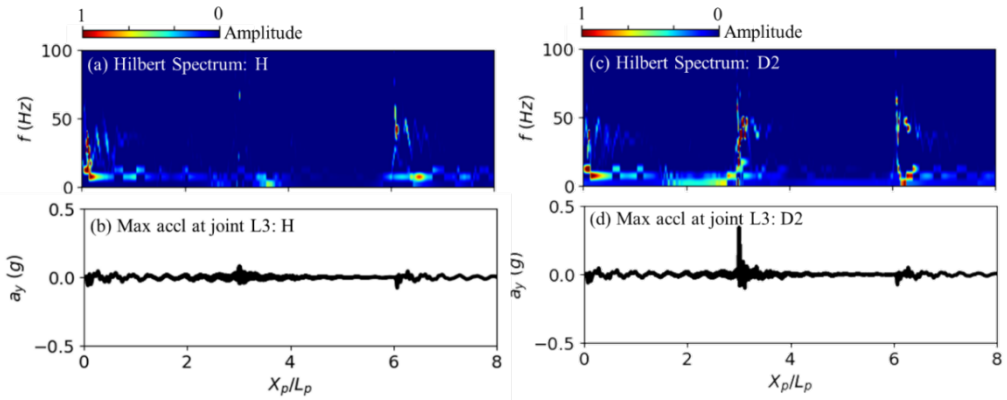

Figure 7. Hilbert spectrum of the acceleration signal at joint L3 for the healthy case H (a,b) compared to the damage case D2 (c,d) plotted versus the location of moving load.

Figures 7(a) and (c) show the plots of the Hilbert spectra (HS) of the acceleration signals (in Figures 7(b) and (d)) at joint L3 for the healthy case H and the damaged case D2. These plots describe the magnitude of energy contained within the given acceleration signals where the magnitude is represented in color, with red having the largest value and blue having the lowest value. It is observed that both the acceleration signals in healthy and damaged cases have a high energy density at their beginning and end, where the load is close to the end supports. The natural frequency of railroad bridge is also increased in these regions. However, the HS plot of the acceleration signal at damage case D2 shows a significant increase in energy density when the load pass through the damage zone at joint L3.

4. DAMAGE CLASSIFICATION

4.1 Machine learning classifiers

Three ML classifiers are evaluated to label the extent of damage in the rail-bridge system:

4.1.1. Support Vector Machine (SVM)

SVM is a ML algorithm mainly employed for classification tasks. The algorithm works by identifying the optimal hyperplane in a high-dimensional feature space that maximizes the margin between the predicted and actual values. This hyperplane is determined using support vectors, a subset of training data points that have the highest margin to the hyperplane. The difference between the predicted and actual values of the support vectors is minimized. SVM is a versatile classification method that can handle complex and high-dimensional datasets. This is accomplished by mapping the input data to a higher-dimensional feature space via a kernel function. The kernel function enables the algorithm to find nonlinear decision boundaries in the feature space without explicitly computing higher-dimensional coordinates [21].

4.1.2. K-Nearest Neighbors (KNN)

KNN is a ML algorithm that may be used in both classification and regression problems. It operates by identifying the K most similar data points in a training dataset, utilizing a distance metric to compute the distance between data points. Subsequently, it labels the new data point by the most common class of its K closest neighbors for classification, or it predicts the average value of the target variable for regression. K-NN is a non-parametric and instance-based learning method that performs well with small datasets, but computational requirements may escalate as dataset size increases [22]

4.1.3. Decision Tree (DT)

DT is a machine learning algorithm that serves both regression and classification tasks. It employs a tree structure comprising nodes, branches, and leaves. The nodes denote features or attributes in the dataset, the branches indicate decision rules, and the leaves hold the output, which can be a numeric value or class label. The algorithm repeatedly splits the data into smaller subsets based on the most informative feature at each node until it satisfies the stopping criterion. DT is a simple and interpretable algorithm that can handle both categorical and numerical data [23].

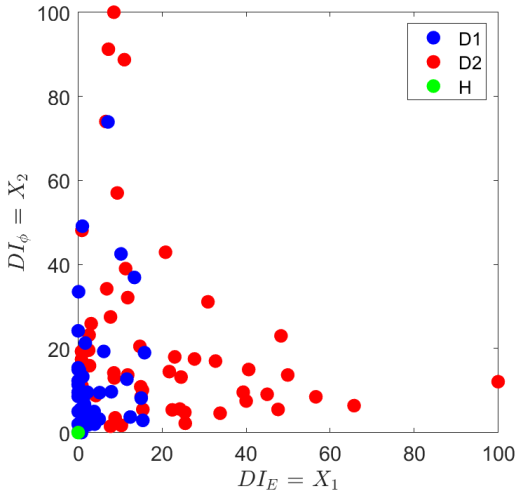

Figure 8. Scatter plot of damage indices for the three different damage labels: healthy (H), damage case 1 (D1), and damage case 2 (D2).

4.2 Results and discussion

The Classification Learner app from MATLAB [24] has been utilized to classify the extent of damage in the rail-bridge system under the given load P=200 kN by varying the speed of moving load from v=15 m/s to v=100 m/s and colleting the generated acceleration signals by sensors mounted at joints U2l, U3, and U2r. The features hidden in dataset were characterized by the two energy and phase damage indices: $X_1=DI_E$ and $X_2=DI_\phi$ for three different classes (damage labels): H, D1, and D2. Figure 8 shows the scatter plot of X_1 versus X_2 for the three different damage labels. The flowchart shown in Figure 9 also demonstrates the process of data generation and damage labeling step by step.

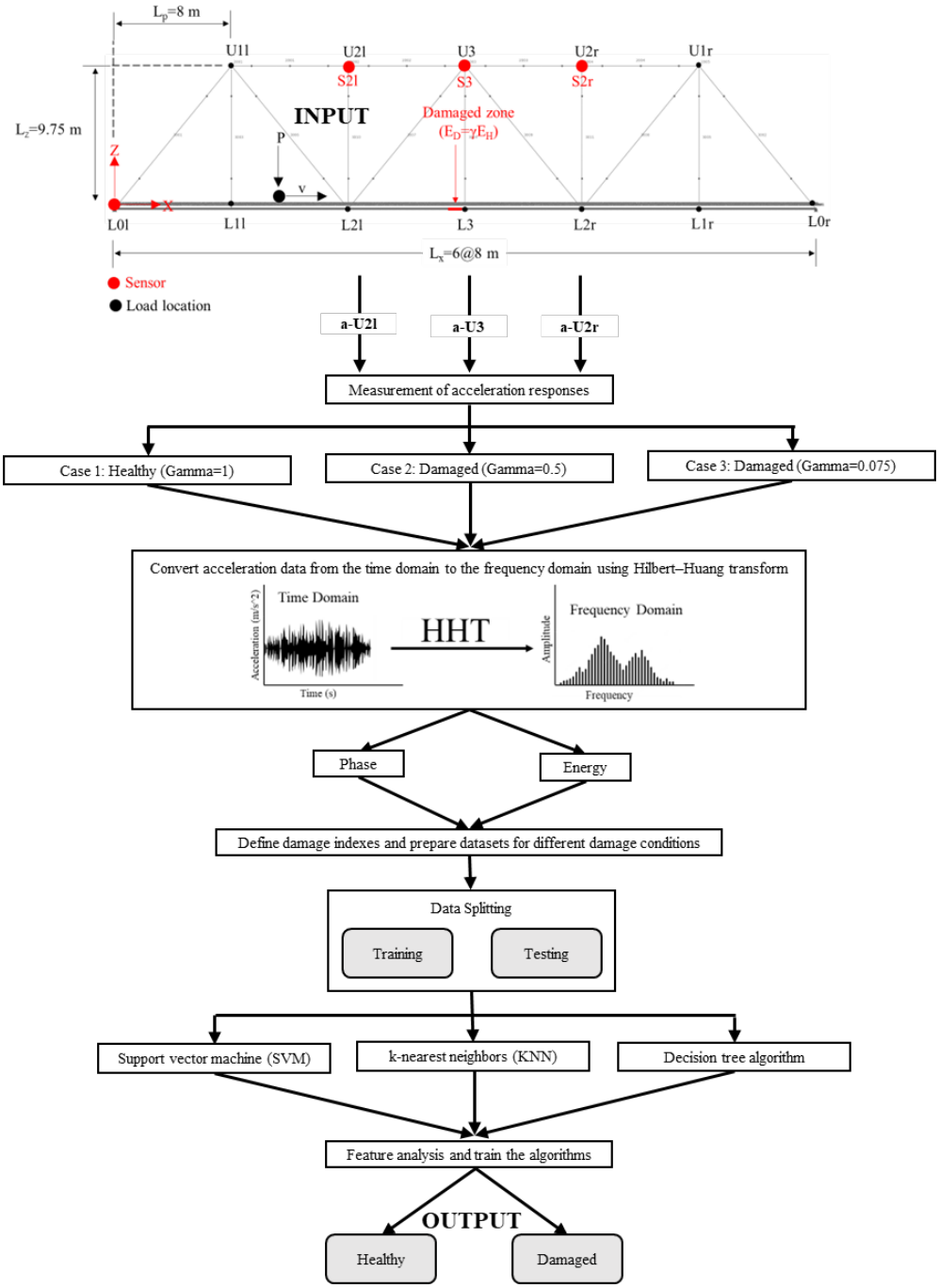

Figure 9. A flowchart to demonstrate the data generation and damage classification process for the given railroad bridge.

The three ML classifiers: SVM, KNN, and DT were used to classify the damage labels by applying a five-fold cross validation (K=5). The ML algorithms were utilized to analyze the dataset with the objective of identifying the algorithm that provides the best classification accuracy. The resulted dataset comprises 204 points, with the algorithm randomly selecting 75% of the data for training and 25% for testing.

Figure 10 shows the confusion matrices for SVM, KNN, and DT algorithms describing the metrics used to evaluate these ML classifiers. Table 1 summarizes the value of these evaluation metrics including: accuracy validation, precision, sensitivity, and F1 value. From all the algorithms, the SVM with the fine Gaussian kernel performed the best in classifying different damage cases from the dataset with 85% accuracy. The fine Gaussian SVM separates data using a narrow Gaussian kernel, yielding a more precise decision boundary. This classifier shows the highest accuracy in terms of precision, sensitivity, and F1 value than the other two classifiers. A higher score in sensitivity analysis from SVM indicates the model effectively identifies actual positive cases. The confusion matrix for SVM shows that around 130 data points were predicted with true positive and negative ratings, approximately 85% of the training dataset the algorithm considers. The DT with a fine kernel scored very close to the SVM with 84.3% accuracy. However, it scored low in terms of sensitivity implying that it cannot correctly identify positive cases while minimizing false negatives.

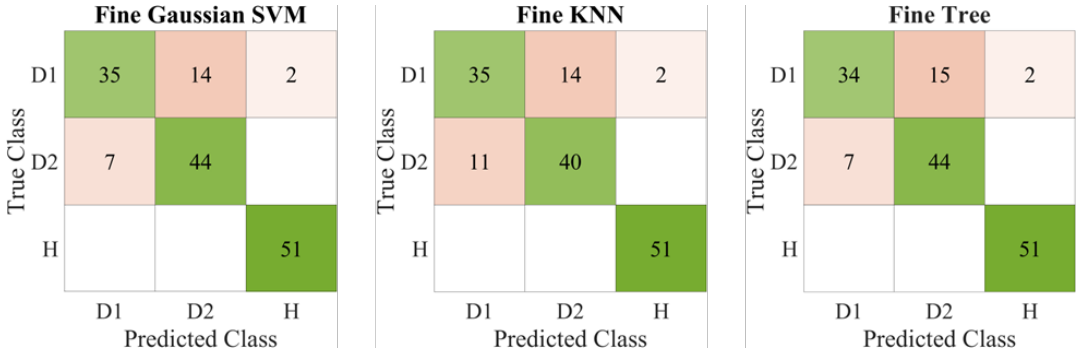

Figure 10. Confusion matrix for SVM, KNN, and DT algorithms.

Table 1. Evaluation metrics for ML classifiers used in the data-analytic study.

ML Classifier	Accuracy Validation	Precision	Sensitivity	F1 Value
		$\frac{TP}{(TP+FP)}$	$\frac{TP}{(TP+FN)}$	$2\times\frac{Precision\times Sensitivity}{Precision+Sensitivity}$
SVM- (Fine Gaussian SVM)	85.0%	83%	83%	75%
Decision tree (Fine tree)	84.3%	76%	69%	72%
K-nearest neighbors (Fine KNN)	82.4%	83%	67%	74%

By comparing the overall performances of ML classifiers used in this study, it can be concluded that the fine Gaussian SVM algorithm is much more capable of classifying the healthy and damage cases from the dataset obtained from the FE model of rail-bridge system.

5. CONCLUSIONS

In this study, a 2D steel truss bridge was modeled by using OpenSEESPy finite element software to study damage to rail-bridge system. Acceleration data for dynamic analysis was generated by placing three sensors at joints U2l, U3, and U2r while running a moving point load across all nodes covering the entire bridge length. Two different damage cases were considered where a change in the steel material's modulus of elasticity, used at the middle section of the bridge, represents the damage. The Hilbert-Huang transform (HHT) was used to convert acceleration data from the time domain to the time-frequency domain to obtain two damage indices: energy and phase. Combining the damage indices marked as damaged case 1 and damaged case 2 along with corresponding damage labels (H, D1, D2), the dataset was constructed to train three different ML classifiers. From the analysis, it can be concluded that SVM is more capable in classifying the damaged and

healthy conditions of the rail-bridge system compared to the other two ML classifiers, namely KNN and DT. It should be, however, mentioned that the damage indices obtained by modeling the damage to the rail are insufficient to get a higher level of accuracy using any of the classifiers employed in the study. Perhaps, a more realistic damage model with meaningful parameters will provide a better result than the one obtained from the simple damage model used in this study. In addition, a 3D FE model, instead of a 2D FE model, with more sensor data will provide a larger dataset to increase the accuracy of ML classifiers which will be the subject of future research of authors.

ACKNOWLEDGEMENTS

This work was supported by the University of Texas Rio Grande Valley. The first and third authors would like to gratefully acknowledge the support and assistance provided to them by the university in terms of Graduate Assistantships and Presidential Research Fellowship Awards.

REFERENCES

[1] "Freight Rail Overview | FRA." https://railroads.dot.gov/rail-network-development/freight-rail-overview (accessed Dec. 13, 2022).

[2] A. S. Nowak Ph D and A. M. Rakoczy Ph D, "Development of System Reliability Models for Railway Bridges," 2012.

[3] S. Reporters, "Train derails over Wabash near downtown Lafayette," *WLFI News 18*. https://www.wlfi.com/news/train-derails-over-wabash-near-downtown-lafayette/article_e87fcf3c-39f4-11ed-a341-7740fc67b6cb.html (accessed Dec. 13, 2022).

[4] "Bridge partially collapses near Phoenix in wake of massive fire and train derailment," *NBC News*. https://www.nbcnews.com/news/us-news/massive-fire-sparked-train-derailment-arizona-n1235191 (accessed Dec. 13, 2022).

[5] "Train derailment on Arkansas River bridge causes traffic back up near Van Buren," *5newsonline.com*, May 08, 2022. https://www.5newsonline.com/article/traffic/train-derailment-on-arkansas-river-bridge-causes-traffic-to-back-up/527-4f021e06-dfdb-4c76-b004-bd3d662e0b2f (accessed Dec. 13, 2022).

[6] "Hampton, Iowa: Union Pacific train derails Monday morning, none injured," *weareiowa.com*, Sep. 04, 2022. https://www.weareiowa.com/article/traffic/hampton-iowa-union-pacific-train-derailment-updates/524-9f93c6ec-fe74-42db-b1c9-dfbc0fbdf1d4 (accessed Dec. 13, 2022).

[7] M. Pokhrel and M. Amjadian, "Damage Detection in an Open-Deck Steel Truss Railroad Bridge under the Train Load using Hilbert-Huang Transform," presented at the Transportation Research Board (TRB) 102nd Annual Meeting, Washington D.C., 2023.

[8] A. Muszynska, "Vibrational diagnostics of rotating machinery malfunctions," *Int. J. Rotating Mach.*, vol. 1, no. 3–4, pp. 237–266, 1995.

[9] S. Beskhyroun, T. Oshima, and S. Mikami, "Wavelet-based technique for structural damage detection," *Struct. Control Health Monit.*, vol. 17, no. 5, pp. 473–494, 2010.

[10] L. Kou, M. Sysyn, S. Fischer, J. Liu, and O. Nabochenko, "Optical Rail Surface Crack Detection Method Based on Semantic Segmentation Replacement for Magnetic Particle Inspection," *Sensors*, vol. 22, no. 21, p. 8214, 2022.

[11] J. Xu, P. Wang, B. An, X. Ma, and R. Chen, "Damage detection of ballast less railway tracks by the impact-echo method," in *Proceedings of the Institution of Civil Engineers-Transport*, 2018, vol. 171, no. 2, pp. 106–114.

[12] D. H. Tobias, D. H. Foutch, and J. Choros, "Investigation of an open deck through-truss railway bridge: work train tests," *Assoc. Am. Railr. Res. Test Dep. Rep. No*, 1993.

[13] M. Zhu, F. McKenna, and M. H. Scott, "OpenSeesPy: Python library for the OpenSees finite element framework," *SoftwareX*, vol. 7, pp. 6–11, Jan. 2018, doi: 10.1016/j.softx.2017.10.009.

[14] D. H. Tobias, D. A. Foutch, and J. Choros, "Loading Spectra for Railway Bridges under Current Operating Conditions," *J. Bridge Eng.*, vol. 1, no. 4, pp. 127–134, Nov. 1996, doi: 10.1061/(ASCE)1084-0702(1996)1:4(127).

[15] D. H. Tobias, "Investigation of an open deck through-truss railway bridge: work train tests," Association of American Railroads Research and Test Department, 1993.

[16] D. Otter, R. Joy, M. C. Jones, and L. Maal, "Need for Bridge Monitoring Systems to Counter Railroad Bridge Service Interruptions," *Transp. Res. Rec.*, vol. 2313, no. 1, pp. 134–143, Jan. 2012, doi: 10.3141/2313-15.

[17] W.-X. Ren and X.-L. Peng, "Baseline finite element modeling of a large span cable-stayed bridge through field ambient vibration tests," *Comput. Struct.*, vol. 83, no. 8–9, pp. 536–550, 2005.

[18] N. E. Huang and Z. Wu, “A review on Hilbert-Huang transform: Method and its applications to geophysical studies,” *Rev. Geophys.*, vol. 46, no. 2, 2008, doi: 10.1029/2007RG000228.
[19] N. Roveri and A. Carcaterra, “Damage detection in structures under traveling loads by Hilbert–Huang transform,” *Mech. Syst. Signal Process.*, vol. 28, pp. 128–144, Apr. 2012, doi: 10.1016/j.ymssp.2011.06.018.
[20] A. A. Mousavi, C. Zhang, S. F. Masri, and G. Gholipour, “Structural Damage Localization and Quantification Based on a CEEMDAN Hilbert Transform Neural Network Approach: A Model Steel Truss Bridge Case Study,” *Sensors*, vol. 20, no. 5, Art. no. 5, Jan. 2020, doi: 10.3390/s20051271.
[21] C. J. Burges, “A tutorial on support vector machines for pattern recognition,” *Data Min. Knowl. Discov.*, vol. 2, no. 2, pp. 121–167, 1998.
[22] T. Cover and P. Hart, “Nearest neighbor pattern classification,” *IEEE Trans. Inf. Theory*, vol. 13, no. 1, pp. 21–27, 1967.
[23] J. R. Quinlan, “Induction of decision trees,” *Mach. Learn.*, vol. 1, pp. 81–106, 1986.
[24] MATLAB R2017b, “MATLAB (R2017b),” *The MathWorks Inc.* 2017. doi: 10.1007/s10766-008-0082-5.